Title

Autoinhibition of Dishevelled protein regulated by its extreme C terminus plays a distinct role in Wnt/β-catenin and Wnt/planar cell polarity (PCP) signaling pathways

Journal

Journal of Biological Chemistry, 292(14)

ISSN

0021-9258

Authors

Qi, Jing
Lee, Ho-Jin
Saquet, Audrey
et al.

Publication Date

2017-04-01

DOI

10.1074/jbc.m116.772509

THE JOURNAL OF BIOLOGICAL CHEMISTRY VOL. 292, NO. 14, pp. 5898–5908, April 7, 2017

Autoinhibition of Dishevelled protein regulated by its extreme C terminus plays a distinct role in Wnt/β-catenin and Wnt/planar cell polarity (PCP) signaling pathways

Received for publication, December 14, 2016, and in revised form, February 19, 2017 Published, JBC Papers in Press, February 21, 2017, DOI 10.1074/jbc.M116.772509

Jing Qi[‡§], Ho-Jin Lee[¶], Audrey Saquet[‖], Xiao-Ning Cheng[‡], Ming Shao[‡], Jie J. Zheng[¶‡‡1], and De-Li Shi[‡‖2]**

*From the [‡]School of Life Sciences, Shandong University, 27 Shanda Nan Road, Jinan 250100, China, the [¶]Department of Structural Biology, St. Jude Children's Research Hospital, Memphis, Tennessee 38105-3678, the **Stein Eye Institute, Department of Ophthalmology, David Geffen School of Medicine at UCLA, Los Angeles, California 90095, the [‡‡]Molecular Biology Institute, UCLA, Los Angeles, California 90095, the [§]Shandong Key Laboratory of Animal Disease Control and Breeding, Institute of Animal Science and Veterinary Medicine, Shandong Academy of Agricultural Sciences, Jinan 250100, China, and the [‖]Institut de Biologie Paris-Seine (IBPS)-Developmental Biology Laboratory, Sorbonne Universités-Université Pierre et Marie Curie (UPMC), University of Paris 06, CNRS UMR7622, 75005 Paris, France*

Edited by Xiao-Fan Wang

Dishevelled (Dvl) is a key intracellular signaling molecule that mediates the activation of divergent Wnt pathways. It contains three highly conserved domains known as DIX, PDZ, and DEP, the functions of which have been well characterized in β-catenin-dependent canonical and β-catenin-independent noncanonical Wnt signaling. The C-terminal region is also highly conserved from invertebrates to vertebrates. However, its function in regulating the activation of different Wnt signals remains unclear. We reported previously that Dvl conformational change triggered by the highly conserved PDZ-binding C terminus is important for the pathway specificity. Here we provide further evidence demonstrating that binding of the C terminus to the PDZ domain results in Dvl autoinhibition in the Wnt signaling pathways. Therefore, the forced binding of the C terminus to the PDZ domain reduces the activity of Dvl in noncanonical Wnt signaling, whereas obstruction of this interaction releases Dvl autoinhibition, impairs its functional interaction with LRP6 in canonical Wnt signaling, and increases its specificity in noncanonical Wnt signaling, which is closely correlated with an enhanced Dvl membrane localization. Our findings highlight the importance of the C terminus in keeping Dvl in an appropriate autoinhibited state, accessible for regulation by other partners to switch pathway specificity. Particularly, the C-terminally tagged Dvl fusion proteins that have been widely used to study the function and cellular localization of Dvl may not truly represent the wild-type Dvl because those proteins cannot be autoinhibited.

The Wnt signaling pathways play a critical role in a wide variety of biological process, including embryonic axis formation, cell proliferation, migration, polarity establishment, and stem cell self-renewal (1–6). Aberrant Wnt signaling leads to tumorigenesis and metastasis of multiple cancer types, in particular, mutations of several key components of the β-catenin-dependent canonical Wnt (Wnt/β-catenin) pathway including adenomatous polyposis coli, β-catenin, and axin have been implicated in colorectal cancer, melanoma, and hepatocellular carcinomas (1, 7–9). The interaction between Wnt ligands and different Frizzled receptors can activate divergent Wnt signaling pathways (10). Dishevelled ((Dvl)[3] or Dsh) protein is a common intracellular mediator that relays different Wnt signals downstream of Frizzled receptors to activate distinct signaling pathways (11). It is composed of three highly conserved domains known as DIX, PDZ, and DEP, which interact with different partners, leading to distinct signaling outcomes (11–14). Both the DIX and PDZ domains are essential for the Wnt/β-catenin pathway (15, 16), whereas the DEP domain is sufficient to activate JNK signaling and has been thought to be involved only in the β-catenin-independent noncanonical Wnt or planar cell polarity (Wnt/PCP) signaling pathway (12, 17–20). Nevertheless, two recent studies suggest that the DEP domain undergoes conformational switch following its interaction with Frizzled receptors and that this is required for Wnt/β-catenin signaling (21, 22). This indicates that Dvl function in the Wnt signaling pathways may be regulated in a more complex manner and that the signaling specificity of Dvl may be conditioned by an appropriate conformation. However, although the DEP domain conformational switch may play a role in signaling to β-catenin (21, 22), whether this influences Wnt/PCP signaling remains to be determined. Thus, how Dvl

This research was supported by Shandong University, Grants 31271556, 31471360, and 31671509 from the National Natural Science Foundation of China, Grant 2015GSF118158 from the Department of Science and Technology of Shandong Province, and by the Groupement des Entreprises Françaises dans la Lutte contre le Cancer (GEFLUC Paris). This work was also supported by National Institutes of Health Grant GM100909 and by Research to Prevent Blindness (to J. J. Z.). The authors declare that they have no conflicts of interest with the contents of this article. The content is solely the responsibility of the authors and does not necessarily represent the official views of the National Institutes of Health.

This article contains supplemental Figs. S1–S5.

[1] To whom correspondence may be addressed: Stein Eye Institute, Dept. of Ophthalmology, David Geffen School of Medicine at UCLA, 100 Stein Plaza, Los Angeles, CA 90095. Tel.: 310-206-2173; E-mail: jzheng@jsei.ucla.edu.

[2] To whom correspondence may be addressed: IBPS-Developmental Biology Laboratory, 9 Quai Saint-Bernard, 75005 Paris, France. Tel.: 442-72772; Fax: 442-73445; E-mail: de-li.shi@upmc.fr.

[3] The abbreviations used are: Dvl, Dishevelled; PCP, planar cell polarity; hpf, hours post-fertilization; DLS, dynamic light scattering; RFP, red fluorescent protein; CE, convergence and extension.

interprets different Wnt signals and triggers distinct cellular responses downstream of Frizzled receptors is still poorly understood (23).

The region C-terminal to the DEP domain of Dvl, in particular the extreme C terminus, is also highly conserved from invertebrates to vertebrates, although it may be relatively divergent in *Drosophila* (24, 25). In addition, despite the presence of distinct features within this region of the three mammalian Dvl proteins (Dvl1, Dvl2, and Dvl3), such as the conserved Dvl3 C-terminal histidine single amino acid repeats that mediate the Wnt5a-stimulated NF-AT-dependent transcriptional response, the last 40 amino acid residues show remarkable conservation among the three isoforms (24, 26). Thus the C-terminal region displays unique primary sequence with many characteristic features potentially implicated in protein interaction and the formation of supermolecular complexes (24). However, its implication in both the Wnt/β-catenin and Wnt/PCP pathways is poorly understood. There is evidence showing that this region binds the third intracellular loop of Frizzled receptors and stabilizes Frizzled-Dvl interaction required for Wnt/β-catenin signaling (27), but how this interaction affects Wnt/PCP signaling remains unclear.

We demonstrated recently that the C terminus of Dvl represents a PDZ-interacting motif that binds to its own PDZ domain and plays a key role in regulating the Wnt signaling pathways (25). In the present study, we provide novel evidence demonstrating that this region regulates the autoinhibition of Dvl in its subcellular localization and signaling activity. We show that the forced binding of the C terminus to the PDZ domain reduces the activity of Dvl in Wnt/PCP signaling, whereas interfering with this interaction enhances Dvl membrane localization and Wnt/PCP signaling. Moreover, our results highlight that C-terminally tagged Dvl proteins have an altered state of autoinhibition and are not regulated in a manner similar to the wild-type protein. In this regard, it is worth noting that C-terminally GFP-tagged Dvl proteins has been widely used to study Wnt signaling in invertebrates (17, 28–30) and vertebrates (31–37), as well as in cultured cell lines (21, 22, 28, 38). These works have contributed strikingly to our understanding of the mechanism of Wnt signaling. Nonetheless, the C-terminally tagged Dvl may behave differently than untagged or N-terminally tagged Dvl in terms of signaling activity and should not be used indiscriminately for the analysis of Dvl function in Wnt signaling in certain circumstances. Indeed, our present study indicates that C-terminally tagged Dvl cooperates less efficiently with the Wnt coreceptor LRP6 in Wnt/β-catenin signaling.

Results

Dvl C terminus differentially regulates the Wnt signaling pathways

Sequence alignment indicates that the C-terminal region of the three Dvl proteins is remarkably conserved among different vertebrate species (Fig. 1*A*). We found previously that deletion of the last eight residues of Xdsh (Dvl2) renders it more active in Wnt/PCP signaling (25), but whether this affects Wnt/β-catenin signaling is not clear. To further understand how the C-terminal region regulates Dvl activity in the Wnt/β-catenin

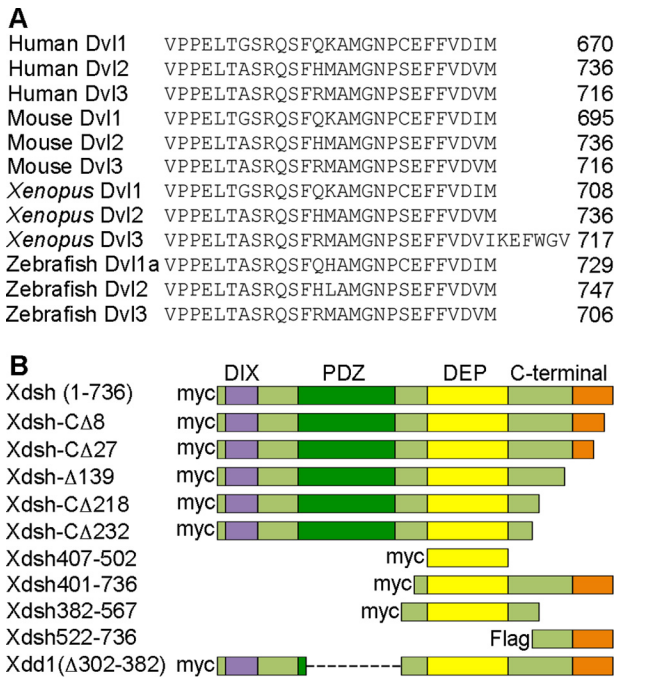

Figure 1. Conservation of Dvl C terminus and generation of Xdsh deletion mutants. *A*, conservation of the Dvl C-terminal region in different vertebrate species. Alignment of the last 33 residues in the extreme C-terminal region of the three Dvl isoforms from different vertebrate species is indicated on the *left*. *B*, schematic representation of wild-type and different Xdsh deletion mutants. The three highly conserved domains, DIX, PDZ, and DEP, as well as the C-terminal region are indicated at the *top*. All constructs are Myc-tagged at the N-terminal region, except for Xdsh522–736, which is FLAG-tagged at the N-terminal region.

and Wnt/PCP pathways, we generated a panel of deletion mutants in *Xenopus* Dvl2 (Fig. 1*B*) and examined their activity in these two Wnt pathways. Transient overexpression of wild-type Xdsh in HEK293 cells induced a robust activation of the TCF/β-catenin-dependent TOPFlash luciferase reporter, whereas transfection of the empty pCS2 vector had no effect. Transfection of a series of Xdsh C-terminal deletion mutants, including Xdsh-CΔ8, Xdsh-CΔ27, Xdsh-CΔ139, Xdsh-CΔ218, and Xdsh-CΔ232, also activated the TOPFlash reporter, but they exhibited a significantly reduced activity in this assay; however the protein level, as verified by Western blotting, was similar to that of wild-type Xdsh (supplemental Fig. S1). By contrast, transfection of other deletion mutants affecting essentially the PDZ domain (Xdsh(407–502), Xdsh(401–736), Xdsh(382–567), Xdsh(522–736), and Xdd1) failed to activate the TOPFlash reporter (supplemental Fig. S1), consistent with the requirement for the PDZ domain in Wnt/β-catenin signaling (15). These results indicate that the C terminus facilitates the activation of the Wnt/β-catenin pathway by Dvl proteins.

To further address the regulatory role of the Dvl C terminus in the Wnt signaling pathways, we first performed a dose-response analysis to compare the activity of Xdsh and Xdsh-CΔ8 in Wnt/β-catenin signaling. Analysis of TOPFlash luciferase reporter activity following transfection of the two constructs in HEK293 cells indicated that, at a similar protein expression level, Xdsh-CΔ8 was less efficient than Xdsh in activating the reporter gene (Fig. 2*A*). This suggests that, to some extent, the absence of the extreme C terminus decreases Dvl activity in

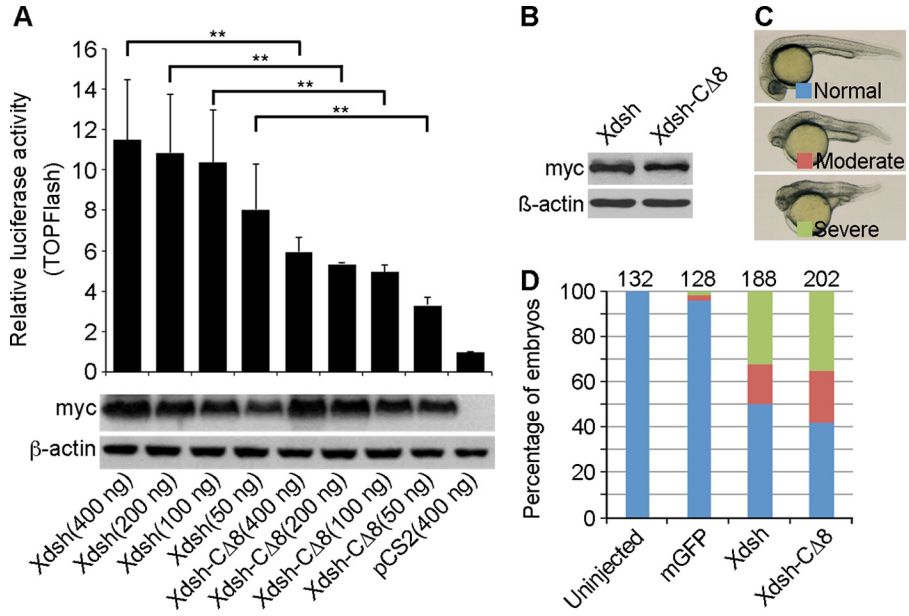

Figure 2. The C terminus differentially regulates Dvl activity in the Wnt signaling pathways. *A*, dose-response analysis to compare the activity between Xdsh and Xdsh-CΔ8 in Wnt/β-catenin signaling in HEK293 cells by TOPFlash reporter assay. Values were expressed relative to the value obtained from empty vector-transfected cells. *Bars* represent the mean values ± S.D. from three independent experiments (**, $p < 0.01$). A representative Western blotting analysis that controls for the protein level is shown under the graph. *B–D*, comparison of defective PCP phenotypes resulted from overexpression of Xdsh and Xdsh-CΔ8 in zebrafish embryos at 24 hpf. *B*, Western blotting analysis to control for the protein level from each injected mRNA. *C*, wild-type and representative PCP phenotypes at 24 hpf. The embryos are grouped into three categories: normal, moderately affected, and severely affected, depending on the extent of axis elongation defects. *D*, statistical analysis of different categories of defective PCP phenotypes. Membrane GFP was used as an injection control. *Numbers* at the *top* of each *stacked column* indicate total embryos scored from four independent experiments using different batches of embryos.

Wnt/β-catenin signaling. In addition, the dose-response analysis also indicated that Xdsh-CΔ8 displayed an obvious difference in activating the TOPFlash reporter when it was transfected at low amounts (between 50 and 100 ng) but not at high amounts (between 100 and 400 ng). This implies that the extreme C terminus may be important in modulating the activity of Dvl when it is present at a low concentration in the cell. We then compared the activity of Xdsh and Xdsh-CΔ8 in Wnt/PCP signaling. Synthetic mRNA (300 pg) was injected into zebrafish embryos at the 1-cell stage, and PCP-defective phenotypes were scored at 24 hpf (hours post-fertilization). From four independent experiments with a protein expression level similar to that verified by Western blotting using 15 randomly selected 24 hpf embryos (Fig. 2*B*), we found that overexpression of Xdsh-CΔ8 was more potent than Xdsh in producing PCP defects, characterized by the occurrence of a higher proportion of embryos with moderately and severely shortened anteroposterior axis (Fig. 2, *C* and *D*), which is a reliable and well characterized phenotypic readout of perturbed Wnt/PCP signaling. These results suggest that the C terminus of Dvl plays a distinct role in the Wnt/β-catenin and Wnt/PCP signaling pathways.

We then performed whole-mount *in situ* hybridization using *ntl* and *dlx3* genes, which label the notochord and the neural plate borders, respectively, as markers to more precisely and quantitatively compare the convergence and extension (CE) defects produced by the overexpression of Xdsh and Xdsh-CΔ8. We also included Xdd1 in this analysis, which was shown to produce specific CE defects when overexpressed in the embryos (15) due to an increased activation of Wnt/PCP signaling (25). At the 100% epiboly stage (10 hpf), a higher proportion of embryos overexpressing Xdsh-CΔ8 or Xdd1 exhibited a broader neural plate as judged by the *dlx3* expression pattern in the neural plate borders (Fig. 3, *A–C* and *G*), indicating that convergence of the neural plate is impaired. The axial mesoderm of these embryos was also shortened and wider, as revealed by the *ntl* expression pattern (Fig. 3, *D–F* and *H*), indicating axis extension defects. All of these phenotypes are characteristic of PCP defects caused by either up-regulation or inhibition of Wnt/PCP signaling (39). Because the C terminus of Dvl can bind to the internal PDZ domain, forming a closed conformation (25), the present result suggests that disruption of this conformation by deleting either the C terminus or the PDZ domain increases Dvl activity in Wnt/PCP signaling and, as a result, enhances PCP phenotype.

Dvl autoinhibition negatively regulates Wnt signaling pathways

Our structural analysis of mouse Dvl1 indicated that the peptide-binding pocket of the PDZ domain could be occupied by its own C terminus (25) and predicted that substitution of the serine residue at position 265 in the PDZ domain and of the isoleucine residue at position 694 (−1) of the C terminus by a cysteine residue could result in a disulfide bond in the PDZ-peptide interaction (Fig. 4). We thus generated a polypeptide, PDZ(S265C)-$(GGS)_3$-DvlC(I694C) named PDZi (supplemental Fig. S2*A*), and examined its conformational change by using the dynamic light scattering (DLS) method. The hydrodynamic radius (R_H) values of PDZ (1.9 ± 0.1 nm) and PDZi (1.5 ± 0.1 nm) are similar, and PDZi is compact because there is no significant change in the R_H value as a function of time. Breaking of the disulfide bond within PDZi by the reducing agent tris(2-carboxyethyl)phosphine resulted in fluctuation of the R_H

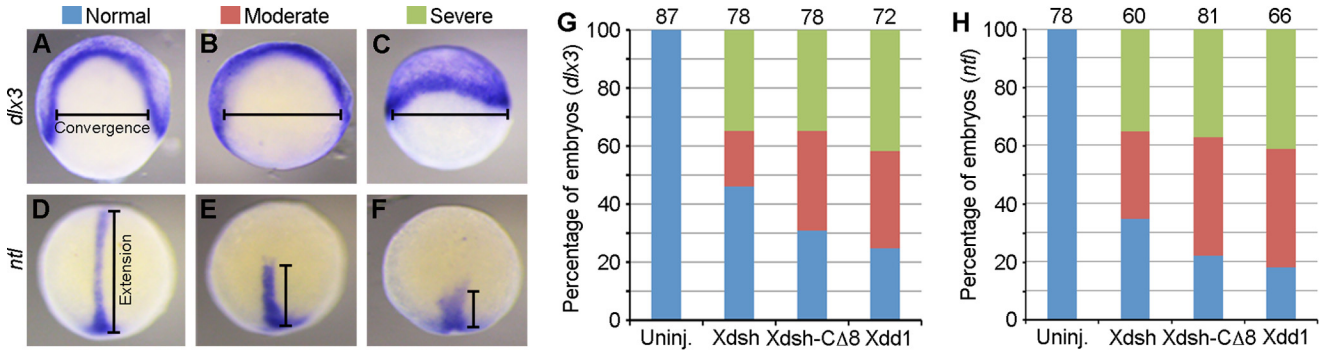

Figure 3. Analysis of CE defects following overexpression of Xdsh, Xdsh-CΔ8 and Xdd1. Zebrafish embryos were injected at the 1-cell stage with synthetic mRNAs encoding Xdsh, Xdsh-CΔ8, or Xdd1, and *in situ* hybridization was performed at bud stage to examine the convergence of the neural plate and the extension of axial mesoderm. The extent of CE defects reflects the activity of Wnt/PCP signaling. *A–F*, representative images of the *dlx3* and *ntl* expression pattern in normal and moderately and severely affected embryos. *G* and *H*, statistical analysis of *dlx3* and *ntl* expression pattern in embryos overexpressing the indicated proteins. *Numbers* at the *top* of each *stacked column* indicate total embryos scored from three independent experiments using different batches of embryos.

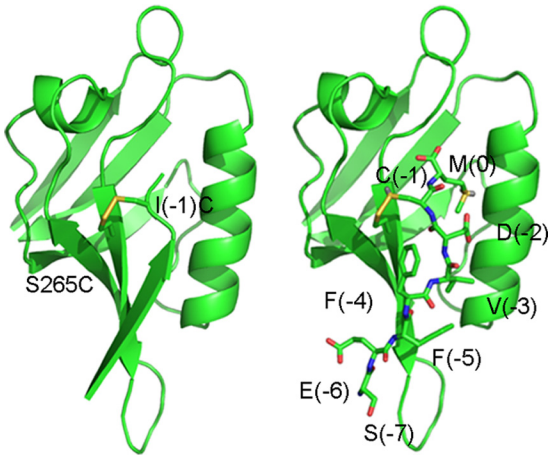

Figure 4. Disulfide bond interaction induces stable Dvl PDZ and C-terminal binding. Structural modeling of a cysteine mutant Dvl1 PDZ (S265C) domain in the disulfide-linked complex with the cysteine mutant C-terminal tail (I694C) shown as a *stick model*. The disulfide bond is shown in *yellow*. Other color codes: *green*, carbon; *red*, oxygen; *blue*, nitrogen.

value of PDZi, indicating the formation of dimer and oligomer (supplemental Fig. 2*B*). The thermal stability of Dvl1 PDZ and PDZi was further investigated as a function of temperature. The result indicated that PDZi was very stable until 90 °C, whereas Dvl1 PDZ was denatured around 57 °C (supplemental Fig. S2*C*). This further indicates that Dvl conformational change can be triggered by the interaction between the extreme C terminus and the PDZ domain.

Based on the above observation, we substituted the serine residue at position 268 in the PDZ domain and the valine residue at position 735 (−1) of the C terminus of Xdsh with a cysteine residue, generating Xdsh268/735C. According to the results obtained with PDZi, we assumed that Xdsh268/735C would form an intramolecular disulfide bond and adopt a closed conformation. As controls, we made a single amino acid change alone, either at position 268 (Xdsh268C) or at position 735 (Xdsh735C). Conversely, we fused the Dvl C terminus with RFP to generate Xdsh-RFP, which should interfere with its binding to PDZ domain, leading to an open conformation (Fig. 5*A*). A TOPFlash reporter assay following transfection in HEK293 cells showed that, at a protein expression level similar to that in Xdsh, Xdsh268/735C was less efficient in activating the reporter gene, and Xdsh-RFP showed a more strongly reduced activity in this assay (Fig. 5*B*). In particular, increasing the amounts of transfected Xdsh-RFP had no obvious effect on the luciferase activity, suggesting that modification of the extreme C terminus strongly affects Dvl activity in Wnt/β-catenin signaling. However, Xdsh268C or Xdsh735C activated the TOPFlash reporter similar to Xdsh (Fig. 5*C*), suggesting that the decreased activity of Xdsh268/735C in Wnt/β-catenin signaling may be a result of intramolecular disulfide bond interaction.

We next examined the activity of Xdsh268/735C and Xdsh-RFP in Wnt/PCP signaling. Analysis by Western blotting of JNK activation following overexpression of these proteins either in HEK293 cells (Fig. 5*D*) or in zebrafish embryos (supplemental Fig. S3) indicated that Xdsh268/735C was less active, whereas Xdsh-RFP was more potent than Xdsh in increasing the p-JNK level. We then overexpressed these proteins in zebrafish embryos by injecting the corresponding mRNA (300 pg) and performed *in situ* hybridization using *ntl* as a marker to determine the notochord shape, which reflects more precisely the PCP phenotype (see Fig. 3, *D–F*). The results from four independent experiments showed that Xdsh268/735C was less effective, whereas Xdsh-RFP was more potent than Xdsh in producing the PCP phenotype, resulting in a higher proportion of embryos with a moderately or severely disrupted *ntl* expression pattern (Fig. 5*E*). These observations suggest that the extent of Dvl autoinhibition mediated by binding of its C terminus to the PDZ domain plays an important regulatory role in the activity of Dvl in different Wnt pathways. More importantly, they indicate that C-terminally tagged Dvl proteins exhibit altered activity with respect to the wild-type Dvl in different Wnt pathways. To further address this issue, we overexpressed the widely used Xdsh-GFP in *Xenopus* embryos to compare its activity with the wild-type Xdsh in inducing PCP defects both in whole embryos and in activin-treated ectoderm explants. It revealed that injection of Xdsh-GFP mRNA (500 pg) in the equatorial region of the two dorsal blastomeres at the 4-cell stage produced a high proportion of embryos with a severely bent and shortened anteroposterior axis, characteristic of the CE-defective phenotype (supplemental Fig. S4, *A–C*). Overexpression of Xdsh-GFP in the ectoderm also strongly impaired activin-induced explant elongation, which mimics CE movements (supplemental Fig. S4, *D–F*). Thus, we conclude

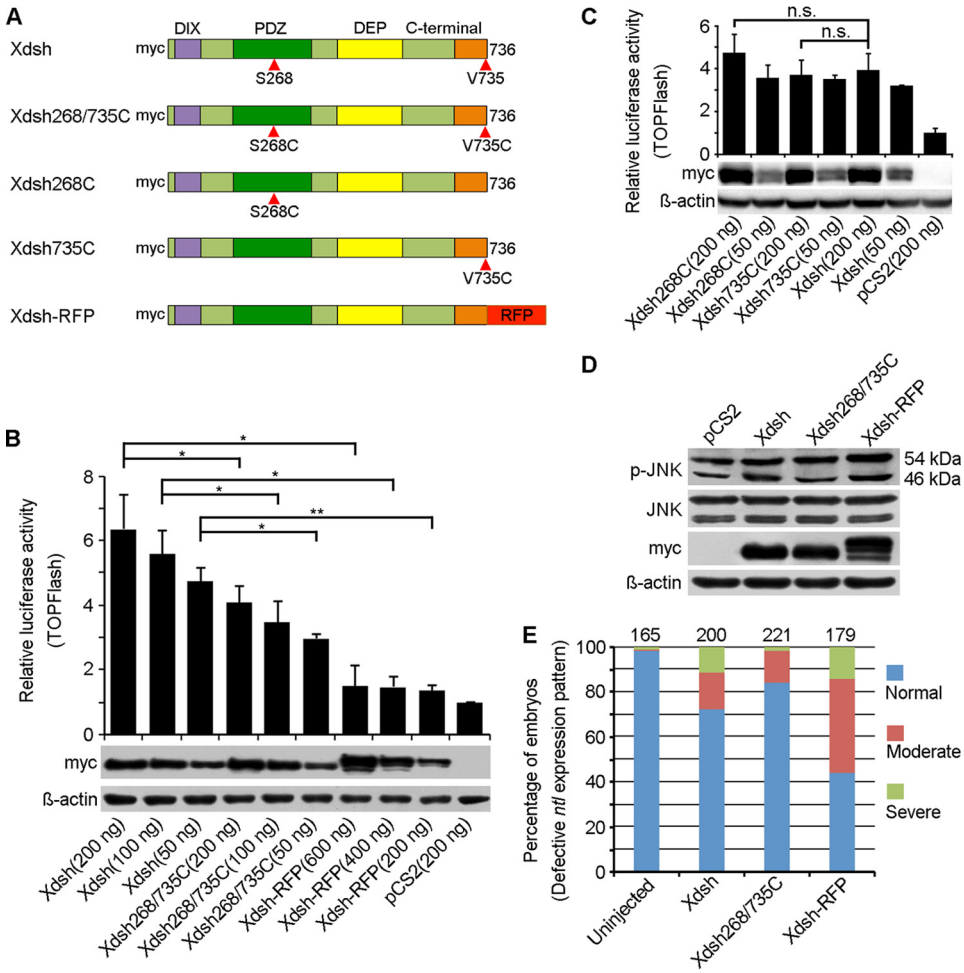

Figure 5. Differential binding of the Dvl C terminus to the PDZ domain results in distinct signaling outcomes. *A*, schematic representation of the indicated constructs. The highly conserved C-terminal region is represented by the *orange color*. *B*, dose-response analysis of the activation of Wnt/β-catenin signaling by Xdsh, Xdsh268/735C, and Xdsh-RFP. Note that Xdsh-RFP shows a strongly reduced activity in Wnt/β-catenin signaling. *C*, dose-response analysis showing that Xdsh268C and Xdsh735C display similar activity to that of Xdsh in Wnt/β-catenin signaling. TOPFlash luciferase reporter assays were performed following transfection of the indicated constructs in HEK293 cells. Values were expressed relative to the value obtained from empty vector-transfected cells. *Bars* represent the mean values ± S.D. from three independent experiments (*, $p < 0.05$; **, $p < 0.01$; *n.s.*, not significant). A representative Western blotting analysis to control for the expression level of different proteins is shown under each graph. *D*, Western blotting analysis of p-JNK level in HEK293 cells following transfection of the indicated constructs. The protein level from transfected constructs was controlled by Western blotting using anti-Myc antibody. Total JNK and β-actin were used as loading controls. *E*, *in situ* hybridization of *ntl* was used to reflect the extent of the defective PCP phenotype in zebrafish embryos at the tail bud stage. Statistical analysis of different categories of PCP phenotype resulted from overexpression of Xdsh, Xdsh268/735C, and Xdsh-RFP. *Numbers* at the *top* of each *stacked column* indicate total embryos scored from four independent experiments using different batches of embryos.

that C-terminally tagged Dvl behaves differently than untagged or N-terminally tagged Dvl in terms of signaling activity.

We further compared the activity of Xdsh, Xdsh268/735C, and Xdsh-RFP in Wnt/β-catenin signaling using the *Xenopus* system, which also provides suitable assays for endogenous Wnt/β-catenin target gene expression and for the extent of axis duplication. Different synthetic mRNAs (500 pg) were injected into the animal pole region at the 2-cell stage, and ectoderm explants were dissected at early gastrula stage for semiquantitative RT-PCR analysis of the expression of *siamois* and *Xnr3*, two early *Xenopus* Wnt/β-catenin target genes. Consistent with the TOPFlash assay in HEK293 cells, the results showed that Xdsh268/735C, and in particular Xdsh-RFP, were less able to induce *siamois* and *Xnr3* expression in ectoderm explants (Fig. 6*A*). Accordingly, they were less efficient than Xdsh in stabilizing the endogenous β-catenin level (Fig. 6, *B* and *C*). In addition, as it has been shown that the activity of the Wnt coreceptors, LRP5 and LRP6, in Wnt/β-catenin signaling is dependent on Wnt-induced phosphorylation (40–44) and requires Dvl function (44), we tested how Xdsh268/735C and Xdsh-RFP cooperate with LRP6 using a *siamois* promoter reporter assay as described previously (25). The reporter (100 pg) was coinjected with synthetic mRNA (200 pg) corresponding to Xdsh, Xdsh268/735C, or Xdsh-RFP in the absence or presence of *LRP6* mRNA (200 pg) in the animal pole region at the 2-cell stage, and a luciferase assay was performed using ectoderm explants dissected at the early gastrula stage. We found that Xdsh significantly synergized with LRP6 to activate the reporter; however, both Xdsh268/735C and Xdsh-RFP were obviously less effective at cooperating with LRP6 (Fig. 6*D*). The same tendency was observed in an axis duplication assay, an *in vivo* readout of Wnt/β-catenin pathway activation. From five independent experiments, a single injection of *LRP6* mRNA (200 pg) into the vegetal region of one ventral blastomere at the

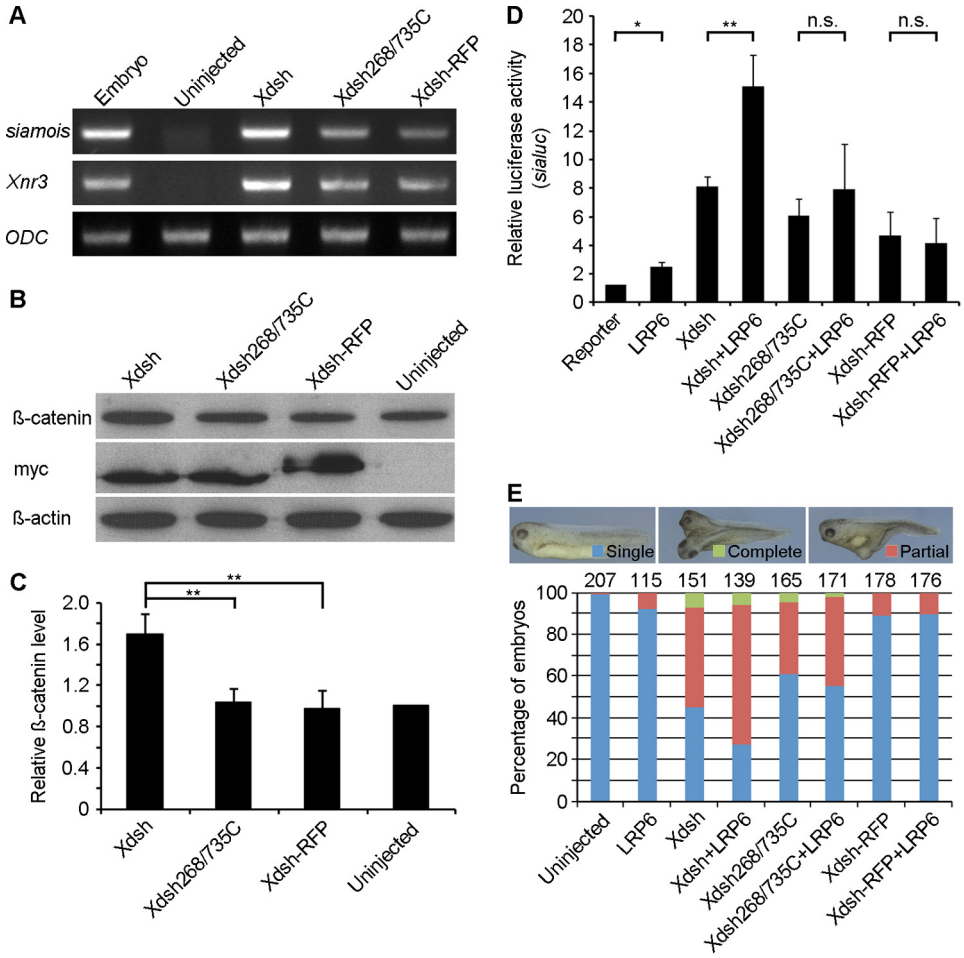

Figure 6. Modification of the extreme C terminus impairs the functional interaction between Dvl and LRP6 in Wnt/β-catenin signaling. *A*, semiquantitative RT-PCR analysis of the expression of Wnt/β-catenin target genes in *Xenopus* ectoderm explants overexpressing Xdsh, Xdsh268/735C, and Xdsh-RFP. *ODC* was used as a loading control. *B*, Western blotting analysis of β-catenin level in *Xenopus* ectoderm explants overexpressing Xdsh, Xdsh268/735C, and Xdsh-RFP. The protein level from injected synthetic mRNA was controlled by Western blotting using anti-Myc antibody, and β-actin was used as a loading control. *C*, quantification of the β-catenin level, normalized to β-actin and β-catenin levels measured in uninjected explants, is set as 1. *Bars* represent the mean values ± S.D. from three independent experiments (**, $p < 0.05$; Student's *t* test). *D*, *siamois* promoter luciferase reporter assay showing the absence of synergistic effect between LRP6 and Xdsh268/735C or Xdsh-RFP. The relative luciferase activity in ectoderm explants injected with the reporter alone is set as 1. *Bars* represent the mean values ± S.D. from three independent experiments (*, $p < 0.05$; **, $p < 0.01$; *n.s.*, not significant). *E*, axis duplication assay showing the absence of functional interaction between LRP6 and Xdsh268/735C or Xdsh-RFP. The embryos were grouped into three categories: single axis, complete secondary axis with head and eyes, and partial secondary axis with absence of head. *Numbers* at the *top* of each *stacked column* indicate total embryos scored from three independent experiments using different batches of embryos.

4-cell stage led to less than 10% of the embryos having a partial secondary axis, whereas a single injection of *Xdsh* mRNA (300 pg) induced the formation of a complete or partial secondary axis in 55% of the embryos. However, the coinjection of *Xdsh* mRNA with *LRP6* mRNA resulted in 73% of the embryos displaying a secondary axis. By contrast, coinjection of the same amounts of *Xdsh268/735C* or *Xdsh-RFP* mRNA with *LRP6* mRNA did not seem to have a synergistic effect (Fig. 6*E*), further indicating that Xdsh268/735C and Xdsh-RFP are less active in Wnt/β-catenin signaling. This observation also implies that Dvl autoinhibition may regulate its functional interaction with the Wnt coreceptor LRP6 in Wnt/β-catenin signaling *in vivo*.

The extreme C terminus influences Dvl activity in Wnt/PCP signaling

We used PDZ-binding small molecules previously to compete with the C terminus of Dvl for binding to the PDZ domain and found that the small molecules enhance Dvl activity in Wnt/PCP signaling (25). In this study, we examined whether the C-terminal region of Dvl itself could induce an open conformation of Dvl and thus enhance PCP phenotype in zebrafish embryos. We expressed increasing amounts of Xdsh alone or along with a given amount of Xdsh(522–736), which retains only the last 215 residues. From three independent experiments, by scoring a large number of embryos, we found that Xdsh(522–736) was able to synergize with low doses of Xdsh to trigger PCP defects. A single injection of 50 pg of *Xdsh* mRNA produced PCP defects in about 20% of the embryos, with moderately and severely shortened anteroposterior axis, whereas a single injection of 200 pg of *Xdsh(522–736)* mRNA produced PCP defects in about 10% of the embryos, indicating that overexpression of Xdsh(522-736) may interfere with endogenous Dvl function. However, more than 40% of the embryos displayed various degrees of PCP-defective phenotypes when the two mRNAs were coinjected (supplemental Fig. S5). A similar synergy was obtained by injecting 100 pg of *Xdsh* mRNA with

200 pg of *Xdsh(522–736)* mRNA, but no obvious synergistic effect was observed when 200 pg of *Xdsh* mRNA was coinjected with 200 pg of *Xdsh(522–736)* mRNA (supplemental Fig. S5). This result suggests that Xdsh(522–736) may prevent Xdsh from forming a closed conformation and, as a consequence, may enhance the activity of Xdsh in Wnt/PCP signaling. It also implies that Dvl would be more sensitive to the regulation by PDZ-binding ligands including its own extreme C terminus when it is present at low concentrations in the cell, whereas this regulation becomes less evident at high concentrations.

Obstructed binding of the C terminus to the PDZ domain enhances Dvl membrane recruitment by frizzled receptor

Membrane relocalization of Dvl is required for activation of the Wnt/PCP pathway (17, 33), but how it is regulated remains unclear (12). Because Xdsh-CΔ8 and Xdsh-RFP were more potent and Xdsh268/735C less active in inducing the PCP phenotype, we wondered how they could be recruited to the plasma membrane by Frizzled receptors. This was analyzed in the zebrafish embryo, which is more appropriate for the detection and observation of membrane localization. N-terminally Myc-tagged Xdsh and different mutants were overexpressed in zebrafish embryos, and their subcellular localization was examined by confocal microscopy following immunostaining using anti-Myc antibody. As reported in previous work (45), Xdsh was essentially distributed in the cytoplasm when overexpressed alone (Fig. 7*A*); however, it was translocated to the membrane when coexpressed with the Frizzled receptor Xfz7 (Fig. 7*B*). Interestingly, Xdsh-CΔ8 exhibited obvious membrane localization even when it was overexpressed alone (Fig. 7*C*), likely through interaction with endogenous Frizzled receptors. The membrane localization of Xdsh-CΔ8 was strongly enhanced in the presence of Xfz7 (Fig. 7*D*). By contrast, Xdsh268/735C was less efficiently recruited to the membrane than Xdsh-CΔ8 in the presence of Xfz7 (Fig. 7, *E* and *F*), which is correlated with its weak activity to induce PCP phenotype. However, like Xdsh-CΔ8, Xdsh-RFP also showed obvious membrane localization in the absence of Xfz7 (Fig. 7*G*), and it was more readily recruited to the membrane in the presence of Xfz7 (Fig. 7*H*). This analysis clearly indicates that the C terminus, depending on the state of its interaction with the PDZ domain, is involved in regulating Dvl subcellular localization, which is required for Wnt/PCP signaling in both invertebrates and vertebrates (17, 33).

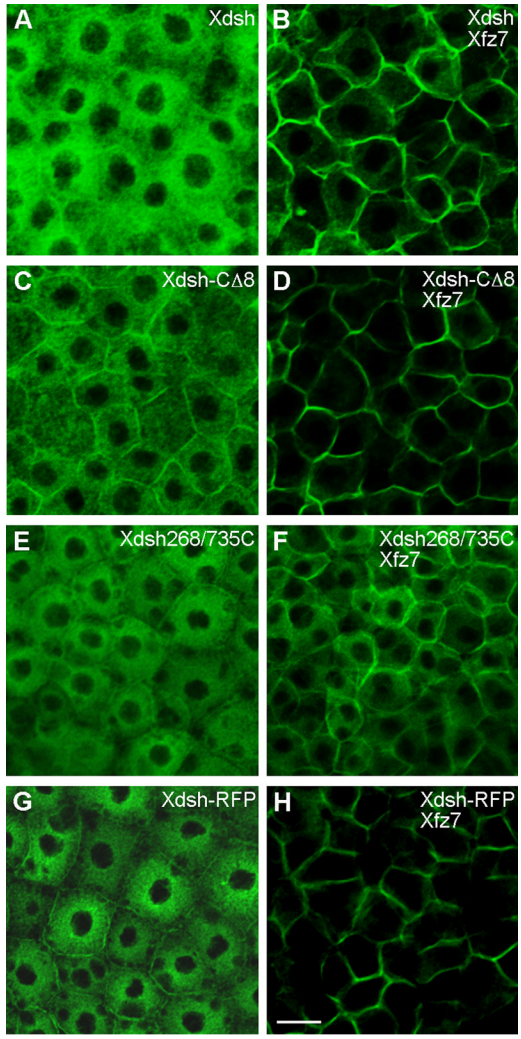

Figure 7. The open conformation of Dvl enhances its membrane recruitment by Frizzled. Representative confocal microscopic analyses of the subcellular distribution of N-terminally Myc-tagged Xdsh and different mutant forms in zebrafish embryonic cells are shown. *A*, Xdsh is localized mainly in the cytoplasm when it is expressed alone. *B*, Xdsh is recruited to the cell membrane in the presence of Xfz7, but cytoplasmic localization is still evident. *C*, Xdsh-CΔ8 is distributed in the cytoplasm, but membrane localization is evident. *D*, in the presence of Xfz7, Xdsh-CΔ8 is strongly recruited to the plasma membrane, resulting in the absence of immunofluorescence staining in the cytoplasm. *E*, Xdsh268/735C localizes to the cytoplasm similarly as Xdsh. *F*, Xdsh268/735C is less efficiently recruited to the cell membrane when coexpressed with Xfz7. *G*, Xdsh-RFP shows obvious membrane localization when it is expressed alone. *H*, coexpression with Xfz7 completely relocalizes Xdsh-RFP to the cell membrane, resulting in the absence of immunofluorescence staining in the cytoplasm. *Scale bar*: 20 μm.

Discussion

In this study, we have demonstrated that the Dvl C terminus regulates Dvl autoinhibition in the Wnt signaling pathways. Stable binding of the C terminus to PDZ domain decreases, whereas obstructed binding increases, Dvl activity in Wnt/PCP signaling. More importantly, we have shown that the open conformation of Dvl is more accessible for membrane localization, which represents a mechanism for the increased Wnt/PCP signaling. Thus, our findings point out that an alteration of the extreme C terminus of Dvl could have an impact on its signaling activity and specificity.

Dvl is an evolutionarily conserved multifunctional scaffold protein. The functional implication of the three highly conserved domains, DIX, PDZ, and DEP, in Wnt/β-catenin and Wnt/PCP signaling has been relatively well characterized and documented (11–13, 46). However, the function of the highly conserved C-terminal region after the DEP domain in these pathways is not clear. There are several studies showing that this region is involved in the regulation of Wnt/β-catenin signaling through interaction with the intracellular loop of Frizzled receptors (27) or through interaction with other partners (24). It has also been demonstrated that the histidine single amino acid repeats that are unique to Dvl3 are essential for Wnt5a-stimulated NF-AT-dependent transcriptional response (26). Recently, we demonstrated that the conserved extreme C terminus binds to the PDZ domain and regulates the conformation change of Dvl, and binding of the C terminus to the PDZ

domain results in a closed conformation, which may negatively influence Wnt/β-catenin signaling (25). However, it remains to be determined exactly how the C terminus of Dvl differentially regulates the Wnt/β-catenin and Wnt/PCP pathways. Using a panel of C-terminal region deletion mutants, we found that removal of the C-terminal region decreased the activity of Dvl in Wnt/β-catenin signaling in a TOPFlash reporter assay, consistent with previous studies (27). On the contrary, the absence of the extreme C terminus or obstruction of its binding to the PDZ domain increased Dvl activity in Wnt/PCP signaling, as revealed by the enhanced PCP defects in zebrafish and *Xenopus* embryos. As the C terminus of Dvl binds to the PDZ domain (25), these observations suggest that the Dvl C terminus may be negatively involved in Wnt/PCP signaling. Further supporting this conclusion, we demonstrated that forced binding of the C terminus to the PDZ domain reduces Dvl activity in Wnt/PCP signaling. This is likely because of its interaction with the PDZ domain, forming a closed conformation (25), which may not be favorable for the interaction of the DEP domain with its partners involved in Wnt/PCP signaling (47–49). Taken together, these observations strongly suggest that the C terminus of Dvl plays a distinct role in different Wnt pathways and may be involved in regulating the pathway specificity of Dvl.

We also compared Dvl C terminus deletion mutants with Xdd1, a PDZ domain deletion mutant that acts as a dominant negative mutant to inhibit Dvl activity in Wnt/β-catenin signaling and induces strong CE defects when expressed in the embryos (15). However, whether the PCP phenotype results from an increase or a decrease in Wnt/PCP signaling has not been elucidated, because it is well established that both activation and inhibition of this pathway produce overall PCP defects (39), although the underlying cell behaviors may be different. Our previous and present studies have solved this issue by showing that the PCP defects caused by overexpression of Xdd1 is associated with an increased JNK activation, which is consistent with a number of previous works showing that the DEP domain is involved in the activation of the Wnt/PCP pathway (17–20). Because deletion of the PDZ domain can also prevent Dvl from forming a closed conformation, it is conceivable that Xdd1 could act as a gain-of-function mutant in Wnt/PCP signaling like the Dvl C terminus deleted forms. Similarly, obstructing the binding of the C terminus to the PDZ domain by its deletion or fusion with RFP or GFP releases Dvl autoinhibition and increases Dvl activity in Wnt/PCP signaling. Taken together, these results further suggest that disruption of the binding between the C terminus and the PDZ domain enhances Dvl activity in Wnt/PCP signaling. In accordance with this conclusion, we showed that coexpression of the Dvl C-terminal region with full-length Dvl could enhance the Dvl-dependent PCP phenotype in zebrafish embryos. Alternatively, we could not exclude the possibility that the free C-terminal fragment may inhibit Dvl activity due to competitive binding to the PDZ domain.

The membrane localization is important for Dvl function in Wnt/PCP signaling (17, 33) but is dispensable for Wnt/β-catenin signaling (33). However, how this is regulated still remains obscure (12). The DEP domain of Dvl plays a critical role in membrane recruitment by Frizzled receptors (17, 27, 50–52). However, the implication of the C terminus in regulating Dvl subcellular localization remains unclear. Interestingly, we found that Dvl mutants in which the interaction between the C terminus and PDZ domain is obstructed exhibited enhanced membrane recruitment by Frizzled receptors. This enhanced membrane localization is closely linked to an increased activity in Wnt/PCP signaling and is consistent with the requirement of Dvl membrane localization in the activation of the Wnt/PCP pathway (17, 33). These findings imply that the C terminus modulates Dvl activity in Wnt/PCP signaling through regulation of its membrane localization. This mechanism has not been identified previously and suggests a functional implication for the Dvl C terminus in regulating Wnt/PCP pathway activation.

It was reported previously that a DEP domain and C-terminal region fragment of Dvl binds the third loop of Frizzled receptors and is required for Wnt/β-catenin signaling; also the C-terminal region is involved in stabilizing the interaction between Frizzled and Dvl (27). This supports a role for the Dvl C-terminal region in regulating Dvl function in the Wnt signaling pathways. It also raises the possibility for an implication of this region in regulating Dvl subcellular localization. We have shown previously that the PDZ domain directly binds a conserved KT*XXX*W motif in the C-terminal region of Frizzled receptors (45, 53). This binding, although relatively weak, may facilitate the membrane recruitment of Dvl by Frizzled receptors. A closed conformation due to occupancy of the PDZ domain by the extreme C terminus (25) may hamper PDZ binding to the KT*XXX*W motif, whereas an open conformation resulting from an obstructed binding between the C terminus and the PDZ domain could facilitate this interaction. It is also plausible that an open conformation would be more favorable for the DEP domain, which is known to play a major role in Dvl localization to the plasma membrane (17, 27, 50–52), to interact with its partners. For example, a charge-dependent interaction of the DEP domain with phospholipids helps to stabilize the direct interaction between Frizzled receptors and *Drosophila* Dsh, which is important for Wnt/PCP pathway selection (52). Thus, this observation supports our present finding that an open conformation of Dvl displays enhanced membrane localization and is more potent in Wnt/PCP signaling. Recently, it has been shown that the interaction of the DEP domain with Frizzled receptors results in a DEP conformational switch, which provides a directional bias for signaling to β-catenin (21, 22). However, whether this conformational switch exerts an influence on Wnt/PCP signaling remains to be determined.

It should be also mentioned that the *Drosophila dsh* null allele can be rescued by C-terminally tagged *Drosophila* Dsh protein (17, 18, 30, 52, 54, 55). This may be because the C terminus of Dsh is less well conserved in *Drosophila*. Indeed, *Drosophila* and vertebrates have divergent C-terminal regions in Dvl proteins, except for the last three amino acids, which resemble a class III PDZ-binding motif in vertebrates but a class II PDZ-binding motif in *Drosophila* (14, 25).

In conclusion, the results obtained in the present work both confirm and extend our previous observation by showing that the extreme C terminus of Dvl differentially regulates Wnt/β-catenin and Wnt/PCP pathway activation. Mechanistically, when the extreme C terminus binds to the PDZ domain, Dvl adopts a closed conformation (25), which could influence the

interaction of both the PDZ and DEP domains with their partners and would constrain the membrane recruitment of Dvl by Frizzled receptors. The binding of the Dvl C terminus to the PDZ domain could occur intramolecularly, but the possibility of intermolecular binding should not be excluded. Nevertheless, both types of binding should result in an open conformation of Dvl, likely dependent on the cell context and local Dvl concentrations within the cell. Thus, our finding suggests that the C terminus of Dvl functions to modulate the activation of both the Wnt/β-catenin and Wnt/PCP pathways. Altogether, our present results strongly implicate the C terminus in Dvl autoinhibition, which should allow the switch of Dvl to a particular pathway depending on the interaction partners. Indeed, our results also suggest that the state of Dvl autoinhibition may influence its functional interaction with the Wnt coreceptor, LRP6; and LRP6 activity in Wnt/β-catenin signaling has been shown to be dependent on Wnt-induced phosphorylation and Dvl function (40–44). Therefore, there is a possibility that C-terminally tagged Dvl proteins display reduced binding to the PDZ domain, resulting in more Dvl proteins with an open conformation. This prevents its functional interaction with LRP6 in Wnt/β-catenin signaling and switches its activity in Wnt/PCP signaling.

Experimental procedures

Mammalian cells

HEK293 cells (ATCC, CRL1573) were cultured in 24-well plates in DMEM supplemented with 10% fetal bovine serum (HyClone), 2 mM L-glutamine, 100 units/ml penicillin, and 100 μg/ml streptomycin in a humidified incubator with 5% CO_2 at 37 °C.

Zebrafish and xenopus embryos

Wild-type zebrafish embryos of the AB strain were produced by natural matings, maintained at 28.5 °C, and staged according to published criteria (56). Procedures for obtaining *Xenopus* embryos and the manipulation of ectoderm explants were as described elsewhere (25, 57). An axis duplication assay was performed by injection of synthetic mRNA into the vegetal region of one ventral blastomere at the 4-cell stage. Analysis of CE defects was performed by injections into the two dorsal blastomeres at the equatorial region of 4-cell stage embryos. Microinjections were performed using a PLI-100A picoliter microinjector (Harvard Apparatus).

Plasmid Constructs and in Vitro Transcription

N-terminally Myc-tagged full-length Xdsh and Xdd1 lacking the PDZ domain were described previously (15). All other Xdsh deletion mutants were generated by PCR amplification, and the PCR products were cloned into the pCS2 vector in-frame with six Myc or two FLAG epitopes. N-terminally Myc-tagged Xdsh268C, Xdsh735C, and Xdsh268/735C, with the serine residue at position 268 and the valine residue at position 735 (−1) substituted by a cysteine residue either individually or simultaneously, were created by site-directed mutagenesis using the QuikChange kit (Stratagene) according to the manufacturer's recommendations. N-terminally Myc-tagged Xdsh-RFP was generated by PCR amplification of Myc-tagged Xdsh and by cloning the PCR product upstream of the RFP sequence in the pCS2 vector. All constructs were sequenced before use. The *Xenopus* Frizzled 7 (Xfz7), Xdsh-GFP, human LRP6, and membrane GFP constructs cloned in the pCS2 vector were described previously (31, 39, 41, 58). The constructs were linearized with Asp-718 or NotI, and capped mRNA were synthesized using a SP6 mMessage Machine kit (Ambion) according to the manufacturer's recommendations.

Expression and purification of Dvl1 PDZ(S265C)-$(GGS)_3$-DvlC(I654C) Fusion Protein

The cDNA encoding PDZ(S265C)-$(GGS)_3$-DvlC(I694C) fusion protein, PDZi, was subcloned into the pET28a vector. The N-terminally His_6-tagged proteins were expressed in BL21(DE3) *Escherichia coli* cells and purified as reported previously (25). In brief, ^{15}N-labeled protein was made by growing transformed cells in MOPS-containing medium with 1 g/liter $^{15}NH_4Cl$. Protein expression was induced by the addition of 1 mM isopropyl 1-thio-β-D-galactopyranoside when the A_{600} of the cells was ~0.6. After 16 h of induction at 16 °C, the cells were resuspended in lysis buffer (20 mM phosphate, 300 mM NaCl, pH 7.8) and sonicated. The lysate was centrifuged, and the supernatant was transferred to a column of nickel-nitrilotriacetic acid beads. After washing with 20 mM imidazole, the protein was eluted by 200 mM imidazole in lysis buffer. The PDZi fusion protein was further purified by chromatography on a Superdex 75-pg column (GE Healthcare) and eluted by 100 mM phosphate buffer, pH 6.5, and 0.5 mM EDTA. The ^{15}N-HSQC spectrum of ^{15}N-labeled PDZi in 100 mM phosphate, pH 6.5, was obtained to confirm whether a disulfide bond would be formed within PDZi.

DLS

The Wyatt DynaPro NanoStar was used to measure the hydrodynamic radius (R_H, nm) of PDZi in a quartz cuvette using 0.1 M PDZi and Dvl1 PDZ in 0.1 M potassium phosphate, pH 6.5. The samples were filtered to eliminate dust particles before performing DLS experiments, and 5 mM tris(2-carboxyethyl)phosphine (Sigma-Aldrich) was used to break the disulfide bond in PDZi protein. DYNAMICS software (Wyatt Technology) was used to analyze the light scattering data.

Immunofluorescence and confocal microscopy

Zebrafish embryos at the 1-cell stage were injected with 100 pg of *Xdsh* or other mutant *Xdsh* mRNA alone or coinjected with 150 pg of *Xfz7* mRNA. They were fixed at the 40% epiboly stage with 4% paraformaldehyde at 4 °C overnight. The vitelline membrane was removed manually, and the embryos were washed three times with TBST (Tris-buffered saline plus 0.1% Triton X-100). They were processed for immunostaining using 9E10 anti-Myc antibody (Santa Cruz Biotechnology) and fluorescein-conjugated secondary antibody as described (59). The samples were analyzed under a confocal microscope (Zeiss LSM700).

Whole-mount in situ hybridization

In situ hybridization was performed on zebrafish embryos at the tail bud stage using *dlx3* and *ntl* probes by standard protocol as described previously (58).

RT-PCR

Xenopus ectoderm explants were dissected at the early gastrula stage from embryos injected previously in the animal pole region with synthetic mRNAs at the 2-cell stage. Total RNA extracted from 20 explants using the guanidine isothiocyanate method was reverse-transcribed as described (60). The PCR primers for *siamois*, *Xnr3*, and ornithine decarboxylase (*ODC*) were reported previously (45).

Western blotting

HEK293 cells at 80% confluence were transfected and cultured for 48 h. They were washed with PBS and lysed in cell lysis buffer consisting of 150 mM NaCl, 50 mM Tris-HCl, pH 7.5, 1% (v/v) Triton X-100, protease inhibitors (1% aprotinin, 0.1% leupeptin, and 2 mM PMSF), and phosphatase inhibitors (PhosSTOP, Roche). Protein extraction from zebrafish embryos was performed as described previously (61). Briefly, 15 embryos were cultured to the appropriate stages and dechorionated manually or through Pronase E treatment. The yolk was disrupted mechanically by gentle pipetting and vortexing. After several washes in Ringer's solutions (116 mM NaCl, 2.9 mM KCl, 1.8 mM $CaCl_2$, and 50 mM HEPES, pH 7.2) to completely remove the yolk, the cell pellets were lysed in extraction buffer (100 mM NaCl, 5 mM EDTA, 0.5% Nonidet P-40, and 10 mM Tris-HCl, pH 7.5) with protease and phosphatase inhibitors. The preparation of protein samples from *Xenopus* ectoderm explants was described previously (45). The samples were resolved by a 10% polyacrylamide gel, transferred onto nitrocellulose membranes, and probed with anti-Myc (Santa Cruz Biotechnology), anti-JNK, anti-p-JNK/SAPK (Cell Signaling), anti-β-catenin (Abcam), or anti-β-actin (Proteintech) antibody in TBS, pH 7.4. Immunolabeled bands were detected using SuperSignal West Pico chemiluminescent substrate (Pierce).

Luciferase assays

HEK293 cells at 80% confluence were transfected with 60 ng of the TOPFlash reporter construct, 6 ng of pRL-TK, and various amounts of different Xdsh constructs or empty vector. At 24–36 h post-transfection, the cells were lysed in 60 μl of lysis buffer (Promega). *Xenopus* embryos injected with different synthetic mRNAs along with the *siamois* promoter reporter DNA (100 pg) were cultured to early gastrula stage, and 10 ectoderm explants were dissected and lysed in 100 μl of lysis buffer. The lysates were clarified by centrifugation, and luciferase activities were measured using a Dual-Luciferase reporter assay kit (Promega) according to the manufacturer's protocol. The values were normalized to *Renilla* luciferase activity, and the results were expressed as relative luciferase activity with respect to empty vector-transfected cells or to *Xenopus* explants injected with the reporter alone.

Statistical analysis

All data were obtained from at least three independent experiments and analyzed using unpaired two-tailed Student's *t* test. *p* values less than 0.05 and 0.01 were considered significant (*) and extremely significant (**), respectively.

Author contributions—J. J. Z. and D. S. conceived and coordinated the work. J. Q., X. C., and M. S. carried out cell and zebrafish studies. H. L. fulfilled the structural analysis. A. S. and D. S. performed the *Xenopus* experiments. J. J. Z. and D. S. wrote the paper. All authors analyzed the data and approved the final version of the manuscript.

Acknowledgments—We thank S. Sokol, X. He, and K. Tamai for providing the plasmid constructs used in this study and the members of our laboratory for technical assistance and helpful discussion.

References

1. Logan, C. Y., and Nusse, R. (2004) The Wnt signaling pathway in development and disease. *Annu. Rev. Cell Dev. Biol.* **20,** 781–810
2. Wang, Y., and Nathans, J. (2007) Tissue/planar cell polarity in vertebrates: new insights and new questions. *Development* **134,** 647–658
3. Angers, S., and Moon, R. T. (2009) Proximal events in Wnt signal transduction. *Nat. Rev. Mol. Cell Biol.* **10,** 468–477
4. Goodrich, L. V., and Strutt, D. (2011) Principles of planar polarity in animal development. *Development* **138,** 1877–1892
5. Singh, J., and Mlodzik, M. (2012) Planar cell polarity signaling: coordination of cellular orientation across tissues. *Wiley Interdiscip. Rev. Dev. Biol.* **1,** 479–499
6. Yang, Y., and Mlodzik, M. (2015) Wnt-Frizzled/planar cell polarity signaling: cellular orientation by facing the wind (Wnt). *Annu. Rev. Cell Dev. Biol.* **31,** 623–646
7. MacDonald, B. T., Tamai, K., and He, X. (2009) Wnt/β-catenin signaling: components, mechanisms, and diseases. *Dev. Cell* **17,** 9–26
8. Clevers, H., and Nusse, R. (2012) Wnt/β-catenin signaling and disease. *Cell* **149,** 1192–1205
9. Anastas, J. N., and Moon, R. T. (2013) WNT signalling pathways as therapeutic targets in cancer. *Nat. Rev. Cancer* **13,** 11–26
10. Niehrs, C. (2012) The complex world of WNT receptor signalling. *Nat. Rev. Mol. Cell Biol.* **13,** 767–779
11. Boutros, M., and Mlodzik, M. (1999) Dishevelled: at the crossroads of divergent intracellular signaling pathways. *Mech. Dev.* **83,** 27–37
12. Wallingford, J. B., and Habas, R. (2005) The developmental biology of Dishevelled: an enigmatic protein governing cell fate and cell polarity. *Development* **132,** 4421–4436
13. Gao, C., and Chen, Y. G. (2010) Dishevelled: the hub of Wnt signaling. *Cell. Signal.* **22,** 717–727
14. Lee, H. J., and Zheng, J. J. (2010) PDZ domains and their binding partners: structure, specificity, and modification. *Cell Commun. Signal.* **8,** 8
15. Sokol, S. Y. (1996) Analysis of Dishevelled signalling pathways during *Xenopus* development. *Curr. Biol.* **6,** 1456–1467
16. Capelluto, D. G., Kutateladze, T. G., Habas, R., Finkielstein, C. V., He, X., and Overduin, M. (2002) The DIX domain targets dishevelled to actin stress fibres and vesicular membranes. *Nature* **419,** 726–729
17. Axelrod, J. D., Miller, J. R., Shulman, J. M., Moon, R. T., and Perrimon, N. (1998) Differential recruitment of Dishevelled provides signaling specificity in the planar cell polarity and Wingless signaling pathways. *Genes Dev.* **12,** 2610–2622
18. Boutros, M., Paricio, N., Strutt, D. I., and Mlodzik, M. (1998) Dishevelled activates JNK and discriminates between JNK pathways in planar polarity and wingless signaling. *Cell* **94,** 109–118
19. Li, L., Yuan, H., Xie, W., Mao, J., Caruso, A. M., McMahon, A., Sussman, D. J., and Wu, D. (1999) Dishevelled proteins lead to two signaling pathways: regulation of LEF-1 and c-Jun N-terminal kinase in mammalian cells. *J. Biol. Chem.* **274,** 129–134
20. Moriguchi, T., Kawachi, K., Kamakura, S., Masuyama, N., Yamanaka, H., Matsumoto, K., Kikuchi, A., and Nishida, E. (1999) Distinct domains of mouse dishevelled are responsible for the c-Jun N-terminal kinase/stress-activated protein kinase activation and the axis formation in vertebrates. *J. Biol. Chem.* **274,** 30957–30962
21. Gammons, M. V., Renko, M., Johnson, C. M., Rutherford, T. J., and Bienz, M. (2016) Wnt signalosome assembly by DEP domain swapping of Dishevelled. *Mol. Cell* **64,** 92–104

22. Gammons, M. V., Rutherford, T. J., Steinhart, Z., Angers, S., and Bienz, M. (2016) Essential role of the Dishevelled DEP domain in a Wnt-dependent human-cell-based complementation assay. *J. Cell Sci.* **129,** 3892–3902
23. Mlodzik, M. (2016) The Dishevelled protein family: still rather a mystery after over 20 years of molecular studies. *Curr. Top. Dev. Biol.* **117,** 75–91
24. Wang, H. Y., and Malbon, C. C. (2012) Dishevelled C terminus: prolyl and histidinyl motifs. *Acta Physiol.* (*Oxf.*) **204,** 65–73
25. Lee, H. J., Shi, D. L., and Zheng, J. J. (2015) Conformational change of Dishevelled plays a key regulatory role in the Wnt signaling pathways. *Elife* **4,** e08142
26. Ma, L., Wang, Y., Malbon, C. C., and Wang, H. Y. (2010) Dishevelled-3 C-terminal His single amino acid repeats are obligate for Wnt5a activation of non-canonical signaling. *J. Mol. Signal.* **5,** 19
27. Tauriello, D. V., Jordens, I., Kirchner, K., Slootstra, J. W., Kruitwagen, T., Bouwman, B. A., Noutsou, M., Rüdiger, S. G., Schwamborn, K., Schambony, A., and Maurice, M. M. (2012) Wnt/β-catenin signaling requires interaction of the Dishevelled DEP domain and C terminus with a discontinuous motif in Frizzled. *Proc. Natl. Acad. Sci. U.S.A.* **109,** E812–E820
28. Tree, D. R., Shulman, J. M., Rousset, R., Scott, M. P., Gubb, D., and Axelrod, J. D. (2002) Prickle mediates feedback amplification to generate asymmetric planar cell polarity signaling. *Cell* **109,** 371–381
29. Weitzel, H. E., Illies, M. R., Byrum, C. A., Xu, R., Wikramanayake, A. H., and Ettensohn, C. A. (2004) Differential stability of β-catenin along the animal-vegetal axis of the sea urchin embryo mediated by dishevelled. *Development* **131,** 2947–2956
30. Singh, J., Yanfeng, W. A., Grumolato, L., Aaronson, S. A., and Mlodzik, M. (2010) Abelson family kinases regulate Frizzled planar cell polarity signaling via Dsh phosphorylation. *Genes Dev.* **24,** 2157–2168
31. Miller, J. R., Rowning, B. A., Larabell, C. A., Yang-Snyder, J. A., Bates, R. L., and Moon, R. T. (1999) Establishment of the dorsal-ventral axis in *Xenopus* embryos coincides with the dorsal enrichment of dishevelled that is dependent on cortical rotation. *J. Cell Biol.* **146,** 427–437
32. Wallingford, J. B., Rowning, B. A., Vogeli, K. M., Rothbächer, U., Fraser, S. E., and Harland, R. M. (2000) Dishevelled controls cell polarity during *Xenopus* gastrulation. *Nature* **405,** 81–85
33. Park, T. J., Gray, R. S., Sato, A., Habas, R., and Wallingford, J. B. (2005) Subcellular localization and signaling properties of Dishevelled in developing vertebrate embryos. *Curr. Biol.* **15,** 1039–1044
34. Wang, J., Hamblet, N. S., Mark, S., Dickinson, M. E., Brinkman, B. C., Segil, N., Fraser, S. E., Chen, P., Wallingford, J. B., and Wynshaw-Boris, A. (2006) Dishevelled genes mediate a conserved mammalian PCP pathway to regulate convergent extension during neurulation. *Development* **133,** 1767–1778
35. Kim, G. H., Her, J. H., and Han, J. K. (2008) Ryk cooperates with Frizzled 7 to promote Wnt11-mediated endocytosis and is essential for *Xenopus laevis* convergent extension movements. *J. Cell Biol.* **182,** 1073–1082
36. Carreira-Barbosa, F., Kajita, M., Morel, V., Wada, H., Okamoto, H., Martinez Arias, A., Fujita, Y., Wilson, S. W., and Tada, M. (2009) Flamingo regulates epiboly and convergence/extension movements through cell cohesive and signalling functions during zebrafish gastrulation. *Development* **136,** 383–392
37. Lee, H. J., Finkelstein, D., Li, X., Wu, D., Shi, D. L., and Zheng, J. J. (2010) Identification of transmembrane protein 88 (TMEM88) as a dishevelled-binding protein. *J. Biol. Chem.* **285,** 41549–41556
38. Ohkawara, B., Glinka, A., and Niehrs, C. (2011) Rspo3 binds syndecan 4 and induces Wnt/PCP signaling via clathrin-mediated endocytosis to promote morphogenesis. *Dev. Cell* **20,** 303–314
39. Djiane, A., Riou, J., Umbhauer, M., Boucaut, J., and Shi, D. (2000) Role of frizzled 7 in the regulation of convergent extension movements during gastrulation in *Xenopus laevis*. *Development* **127,** 3091–3100
40. Tamai, K., Zeng, X., Liu, C., Zhang, X., Harada, Y., Chang, Z., and He, X. (2004) A mechanism for Wnt coreceptor activation. *Mol. Cell* **13,** 149–156
41. Zeng, X., Tamai, K., Doble, B., Li, S., Huang, H., Habas, R., Okamura, H., Woodgett, J., and He, X. (2005) A dual-kinase mechanism for Wnt co-receptor phosphorylation and activation. *Nature* **438,** 873–877
42. Bilic, J., Huang, Y. L., Davidson, G., Zimmermann, T., Cruciat, C. M., Bienz, M., and Niehrs, C. (2007) Wnt induces LRP6 signalosomes and promotes dishevelled-dependent LRP6 phosphorylation. *Science* **316,** 1619–1622
43. Zeng, X., Huang, H., Tamai, K., Zhang, X., Harada, Y., Yokota, C., Almeida, K., Wang, J., Doble, B., Woodgett, J., Wynshaw-Boris, A., Hsieh, J. C., and He, X. (2008) Initiation of Wnt signaling: control of Wnt coreceptor Lrp6 phosphorylation/activation via frizzled, dishevelled and axin functions. *Development* **135,** 367–375
44. MacDonald, B. T., Yokota, C., Tamai, K., Zeng, X., and He, X. (2008) Wnt signal amplification via activity, cooperativity, and regulation of multiple intracellular PPPSP motifs in the Wnt co-receptor LRP6. *J. Biol. Chem.* **283,** 16115–16123
45. Umbhauer, M., Djiane, A., Goisset, C., Penzo-Méndez, A., Riou, J. F., Boucaut, J. C., and Shi, D. L. (2000) The C-terminal cytoplasmic Lys-Thr-*X*-*X*-*X*-Trp motif in frizzled receptors mediates Wnt/β-catenin signalling. *EMBO J.* **19,** 4944–4954
46. He, X., and Axelrod, J. D. (2006) A WNTer wonderland in Snowbird. *Development* **133,** 2597–2603
47. Angers, S., Thorpe, C. J., Biechele, T. L., Goldenberg, S. J., Zheng, N., MacCoss, M. J., and Moon, R. T. (2006) The KLHL12-Cullin-3 ubiquitin ligase negatively regulates the Wnt-β-catenin pathway by targeting Dishevelled for degradation. *Nat. Cell Biol.* **8,** 348–357
48. Habas, R., Kato, Y., and He, X. (2001) Wnt/Frizzled activation of Rho regulates vertebrate gastrulation and requires a novel Formin homology protein Daam1. *Cell* **107,** 843–854
49. Liu, W., Sato, A., Khadka, D., Bharti, R., Diaz, H., Runnels, L. W., and Habas, R. (2008) Mechanism of activation of the Formin protein Daam1. *Proc. Natl. Acad. Sci. U.S.A.* **105,** 210–215
50. Rothbächer, U., Laurent, M. N., Deardorff, M. A., Klein, P. S., Cho, K. W., and Fraser, S. E. (2000) Dishevelled phosphorylation, subcellular localization and multimerization regulate its role in early embryogenesis. *EMBO J.* **19,** 1010–1022
51. Wong, H. C., Mao, J., Nguyen, J. T., Srinivas, S., Zhang, W., Liu, B., Li, L., Wu, D., and Zheng, J. (2000) Structural basis of the recognition of the dishevelled DEP domain in the Wnt signaling pathway. *Nat. Struct. Biol.* **7,** 1178–1184
52. Simons, M., Gault, W. J., Gotthardt, D., Rohatgi, R., Klein, T. J., Shao, Y., Lee, H. J., Wu, A. L., Fang, Y., Satlin, L. M., Dow, J. T., Chen, J., Zheng, J., Boutros, M., and Mlodzik, M. (2009) Electrochemical cues regulate assembly of the Frizzled/Dishevelled complex at the plasma membrane during planar epithelial polarization. *Nat. Cell Biol.* **11,** 286–294
53. Wong, H. C., Bourdelas, A., Krauss, A., Lee, H. J., Shao, Y., Wu, D., Mlodzik, M., Shi, D. L., and Zheng, J. (2003) Direct binding of the PDZ domain of Dishevelled to a conserved internal sequence in the C-terminal region of Frizzled. *Mol. Cell* **12,** 1251–1260
54. Axelrod, J. D. (2001) Unipolar membrane association of Dishevelled mediates Frizzled planar cell polarity signaling. *Genes Dev.* **15,** 1182–1187
55. Yanfeng, W. A., Berhane, H., Mola, M., Singh, J., Jenny, A., and Mlodzik, M. (2011) Functional dissection of phosphorylation of Disheveled in *Drosophila*. *Dev. Biol.* **360,** 132–142
56. Kimmel, C. B., Ballard, W. W., Kimmel, S. R., Ullmann, B., and Schilling, T. F. (1995) Stages of embryonic development of the zebrafish. *Dev. Dyn.* **203,** 253–310
57. Li, H. Y., Grifone, R., Saquet, A., Carron, C., and Shi, D. L. (2013) The Xenopus homologue of Down syndrome critical region protein 6 drives dorsoanterior gene expression and embryonic axis formation by antagonising polycomb group proteins. *Development* **140,** 4903–4913
58. Cao, J. M., Li, S. Q., Zhang, H. W., and Shi, D. L. (2012) High mobility group B proteins regulate mesoderm formation and dorsoventral patterning during zebrafish and *Xenopus* early development. *Mech. Dev.* **129,** 263–274
59. Cao, J., Li, S., Shao, M., Cheng, X., Xu, Z., and Shi, D. (2014) The PDZ-containing unconventional myosin XVIIIA regulates embryonic muscle integrity in zebrafish. *J. Genet. Genomics* **41,** 417–428
60. Li, H. Y., Bourdelas, A., Carron, C., and Shi, D. L. (2010) The RNA-binding protein Seb4/RBM24 is a direct target of MyoD and is required for myogenesis during *Xenopus* early development. *Mech. Dev.* **127,** 281–291
61. Shao, M., Liu, Z. Z., Wang, C. D., Li, H. Y., Carron, C., Zhang, H. W., and Shi, D. L. (2009) Down syndrome critical region protein 5 regulates membrane localization of Wnt receptors, Dishevelled stability and convergent extension in vertebrate embryos. *Development* **136,** 2121–2131